Supplementary Information

*H migration-assisted MvK mechanism for efficient electrochemical NH$_3$ synthesis over TM-TiNO

Luyao Cui[a], Zijun Sun[d], Yawen Wang[a], Xuan Jian[c], Houfen Li[b], Xiao Zhang[b], Xiaoming Gao[c],

Rui Li[a,b,*], Jianxin Liu[a,**]

[a] *Key Laboratory of Coal Science and Technology Ministry of Education, College of Chemical*

Engineering and Technology, Taiyuan University of Technology, Taiyuan 030024, Shanxi, China

[b] *Shanxi Key Laboratory of Compound Air Pollutions Identification and Control, College of*

Environmental Science and Engineering, Taiyuan University of Technology Taiyuan 030024,

Shanxi, China

[c] *College of Chemistry and Chemical Engineering, Shaanxi Key Laboratory of Chemical Reaction*

Engineering, Yan'an University, Yan'an 716000, Shaanxi, China

[d] *Xi'an North Huian Chemical Industries Co. Ltd, Xi'an 710302, Shaanxi, China*
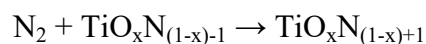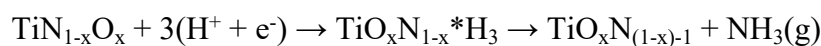
*Corresponding authors.

E-mail addresses: liujx0519@163.com (J. X. Liu), lirui13233699182@163.com (R. Li);

For the construction of the RS-TiN$_{1-x}$O$_x$ model, we use an alternative compositional approach by substituting O into the pristine RS-TiN unit cell, comprising 4 Ti and 4 N. Combining the high crystal symmetry, the octahedral face-centered cubic crystal system are obtained in Fig.S1a. When the value of x is 0.25, 0.50, and 0.75, the adjacent vacancies are filled alternatively with 3, 2, and 1 N, along with the corresponding substituted O. Moreover, TiN functions as a conductor, allowing the Ti_3d electrons in the conduction band to transfer to the O atoms. This stabilizes the model without requiring external electron sources.
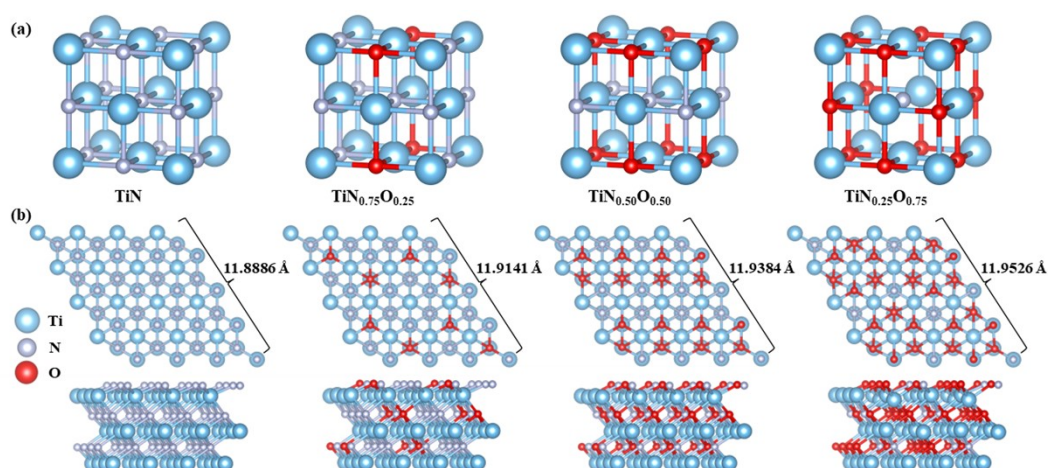
Fig. S1. (a) Unit cell crystal structures of non-stoichiometric RS-TiN$_{1-x}$O$_x$; (b) Side and top views of a 6 atomic layer slab configuration of TiN$_{1-x}$O$_x$ (111)

$$TiN_{1-x}O_x + 3(H^+ + e^-) \rightarrow TiO_xN_{1-x}*H_3 \rightarrow TiO_xN_{(1-x)-1} + NH_3(g)$$

$$N_2 + TiO_xN_{(1-x)-1} \rightarrow TiO_xN_{(1-x)+1}$$

$$TiO_xN_{(1-x)+1} + 3(H^+ + e^-) \rightarrow TiO_xN_{(1-x)+1}*H_3 \rightarrow TiN_{1-x}O_x + NH_3(g)$$

$$H_2O + * \rightarrow *OH + (H^+ + e^-)$$

Scheme S1. The Mar-van Krevelen mechanism for ammonia synthesis on TiN$_{1-x}$O$_x$

| TM-TiNO	Magnetic moment (μB)	TM-TiNO	Magnetic moment (μB)
Fe-TiNO	2.766	Co-TiNO	-0.350
Ni-TiNO	0.760	Ru-TiNO	0.038
Rh-TiNO	0.307	Pd-TiNO	-0.080
Os-TiNO	0.414	Ir-TiNO	0.228

Table S1. The ground state magnetic moment of the average TM atoms in TM-TiNO systems (in Bohr magnetons, μB)

|	Formation energy (eV)			Adsorption energy (eV)	
	E_{for-Nv}	E_{for-Ov}	$E_{for-Tiv}$	N_2	H_2O
$TiN_{0.75}O_{0.25}$	2.020	3.020	5.337	-	-
$TiN_{0.50}O_{0.50}$	1.932	2.832	2.936	-	-
$TiN_{0.25}O_{0.75}$	1.535	2.314	1.351	-	-
$TiNO^SN_{lattice}$	1.387	2.993	1.950	-0.170	-0.211
TiNO-Nv	-	-	-	-1.219	-0.991
Fe-TiNO	1.044	3.004	2.110	-1.406	-0.928
Co-TiNO	1.151	2.837	2.180	-0.849	-0.843
Ni-TiNO	0.811	2.940	1.679	-0.512	-0.727
Ru-TiNO	1.087	2.990	2.165	-1.080	-0.909
Rh-TiNO	1.062	2.872	1.800	-0.752	-0.719
Pd-TiNO	1.065	2.909	3.223	-0.829	-0.495
Os-TiNO	1.064	3.017	2.087	-1.668	-0.921
Ir-TiNO	0.996	2.891	1.847	-1.471	-1.633

Table S2. The formation energy of surface Nv, Ov, and Tiv, and the adsorption energy of N_2 and H_2O in TM-TiNO systems
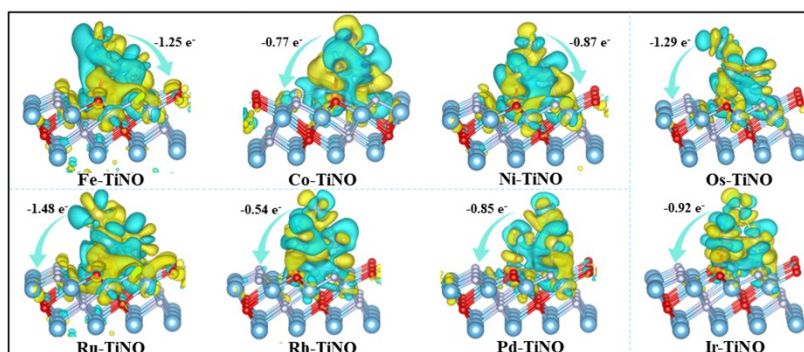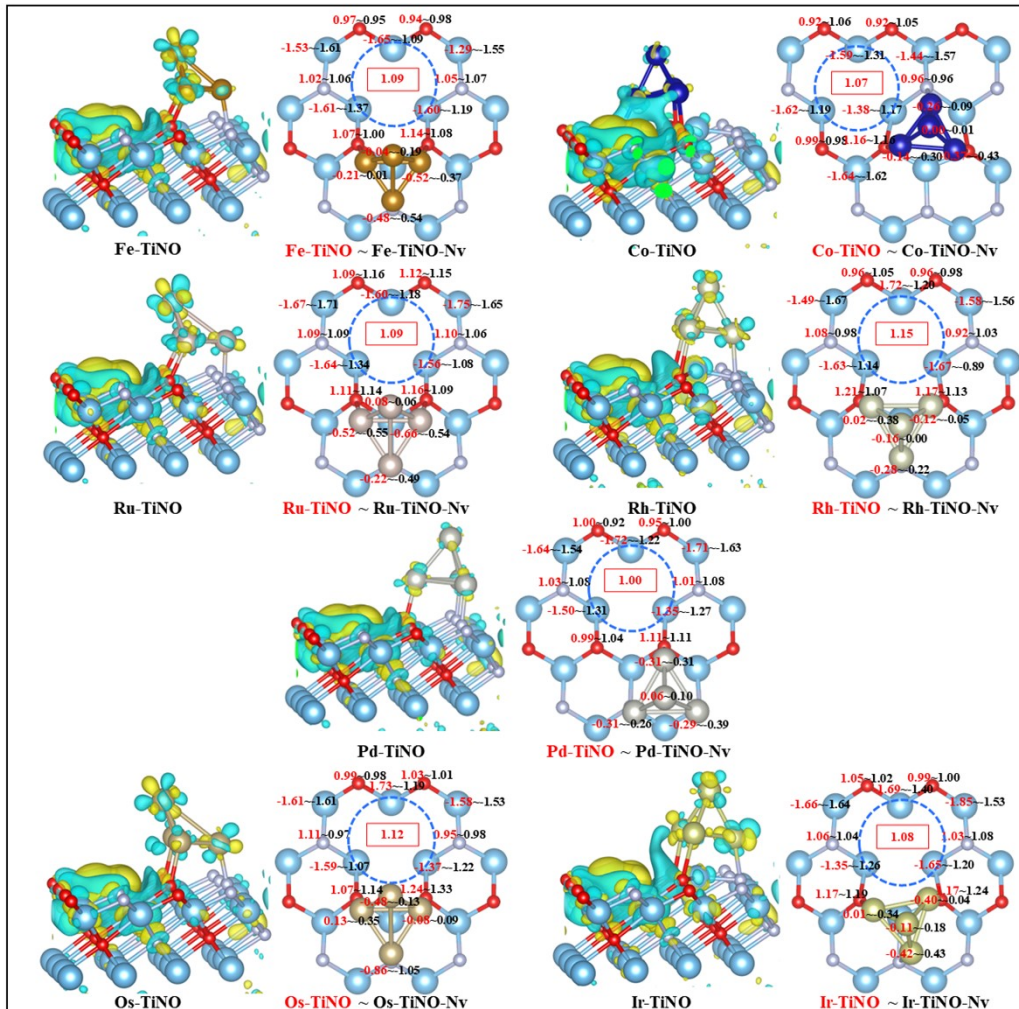

Fig. S2. The corresponding charge density difference (the isosurface is 0.001 e/Bohr^3, cyan and yellow represent charge loss and accumulation, respectively)
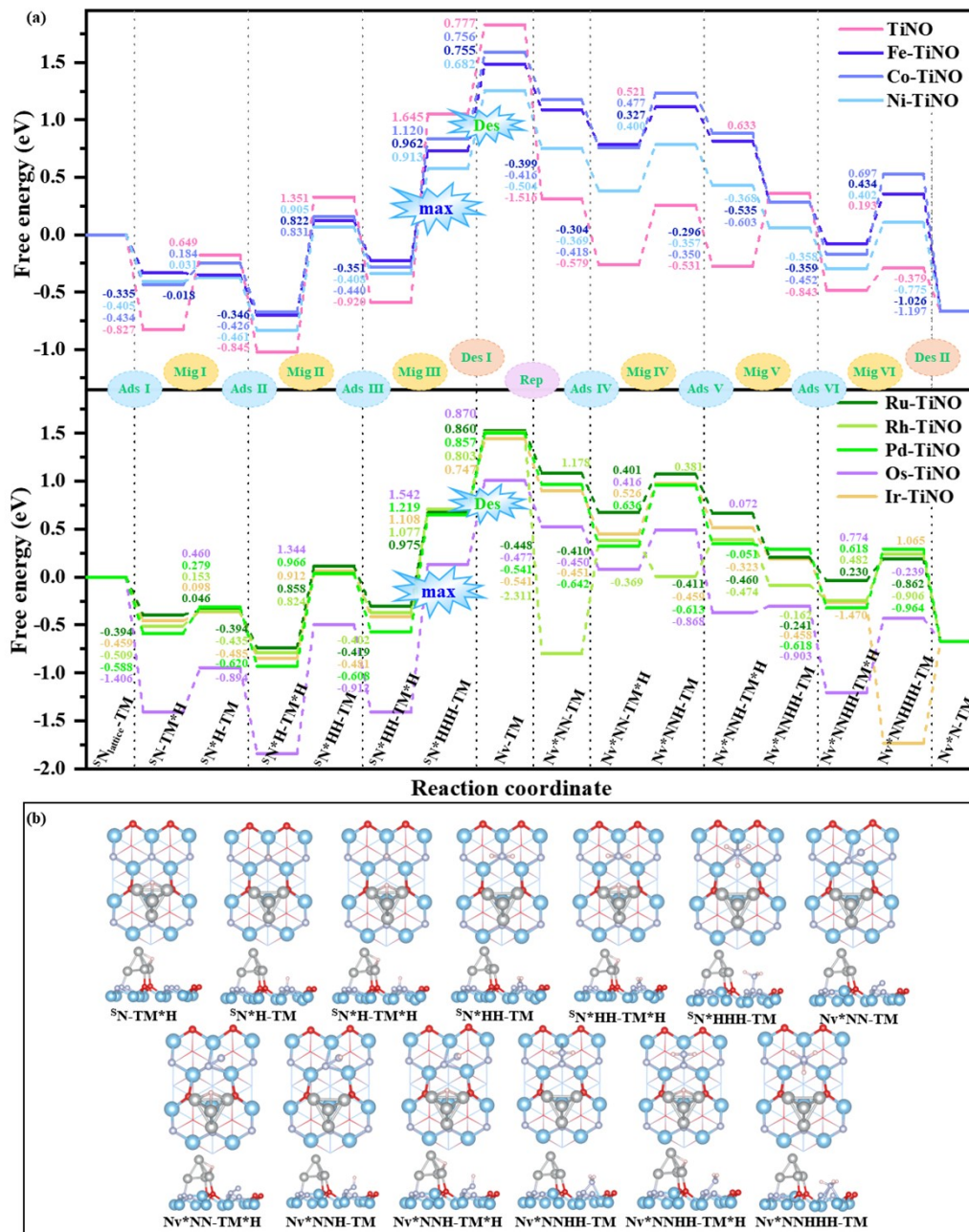
Fig. S3. (a) The ΔG diagram for the ENRR via *H migration-assisted MvK mechanism on TM-TiNO. (b) The corresponding structures for the ENRR via *H migration-assisted MvK mechanism on TM-TiNO
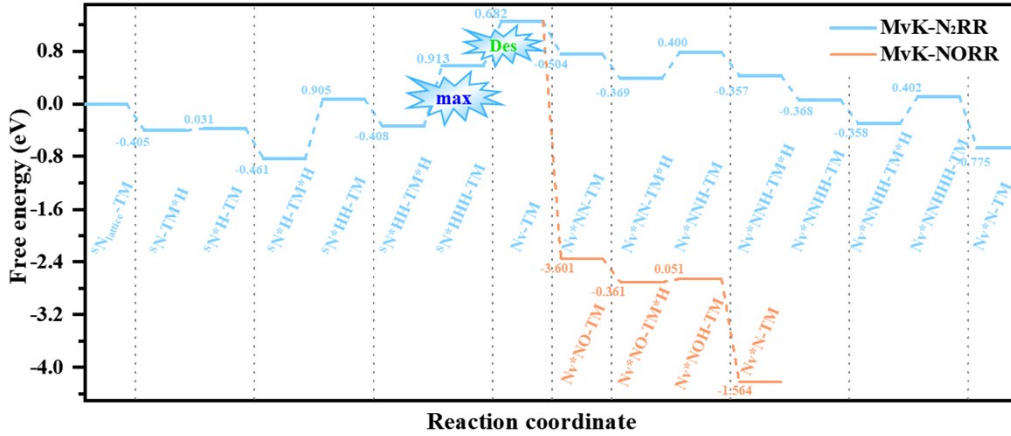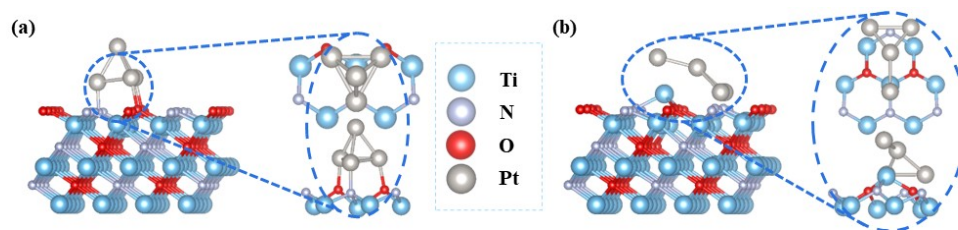
Fig. S4. The ΔG diagram for the EN_2RR and ENORR via *H migration-assisted MvK mechanism on Ni-TiNO

Fig. S5. The CDD at the $^SN_{lattice}$ position of TM-TiNO (the isosurface is 0.001 e/Bohr³, and cyan and yellow represent charge loss and accumulation, respectively) and the

Bader charge of TM-TiNO ~ TM-TiNO-Nv (the values are shown in red ~ black, respectively)

Fig. S6. (a) The initial and (b) optimized structure of Pt-TiNO